

Aggregation of self-propelled colloidal rods near confining walls

H. H. Wensink* and H. Löwen†

*Institut für Theoretische Physik II: Weiche Materie,
Heinrich-Heine-Universität Düsseldorf, Universitätsstraße 1, D-40225 Düsseldorf, Germany*

(Dated: November 3, 2018)

Non-equilibrium collective behavior of self-propelled colloidal rods in a confining channel is studied using Brownian dynamics simulations and dynamical density functional theory. We observe an aggregation process in which rods self-organize into transiently jammed clusters at the channel walls. In the early stage of the process, fast-growing hedgehog-like clusters are formed which are largely immobile. At later stages, most of these clusters dissolve and mobilize into nematized aggregates sliding past the walls.

PACS numbers: 82.70.Dd, 05.40.-a, 61.20.Lc, 61.30.-v

Swimming microorganisms, insects, birds and fish frequently move collectively in large groups with spontaneous liquid crystalline order. Considerable recent research activity has been devoted to understand the origin of flocks and swarms in terms of simple models of self-propelled particles [1, 2, 3, 4, 5, 6, 7, 8]. In these models, “active” rods are driven by their own motor along the rod orientation axis and dissipate energy in the suspending medium. In fact, it has been shown that a local interaction between neighboring particles which favors mutual alignment induces a non-equilibrium phase transition from a state of zero transport to another one involving a big swarm with cooperative transport [1]. This nematically ordered state has been analyzed with hydrodynamic approaches [4] and instabilities at large wavelengths and giant density fluctuations were predicted [4, 7, 8]. In a model with explicit rod interactions, self-organized vortex clusters were found in which particles rotate around a common center [3, 5].

Recently self-propelled rods have been realized in fluidized monolayers of macroscopic rods [9] and by means of vibrating asymmetric granular rods [10]. Giant density fluctuation were confirmed [9]. In these realizations, the rod-rod interaction is the crucial input in contrast to collective motions of bacteria or low-Reynolds-number micro-swimmers [11] which are dominated by hydrodynamic interactions [12, 13]. While most investigations have been performed in the bulk, mainly in two spatial dimensions (2D), there are few studies of self-propelled rods in confinement. Micro-swimmers moving in channels have been investigated in Ref. 14. Self-propelled granular rods in circular-shaped cells were studied experimentally in Ref. 9 and clustering of particles near the cell boundaries was found [10].

In this paper we study the effect of channel confinement on the collective behavior of self-propelled inter-

acting colloidal rods by means of Brownian dynamics computer simulation and dynamical density functional theory. Our motivation to do so is threefold: First, since every realization in nature is finite, there is a general need to clarify the collective behavior of active rods close to system boundaries, and, in particular, to feature the transport properties of colloidal particles. Second, transport through narrow channels is omnipresent in many realizations, e.g. the propagation of microorganisms through veins and pores. Third, a predictive theory which starts on the level of the interactions and incorporates microscopic correlations is needed.

A 2D slit will cause the rods to align along the channel walls such that a nematized steady state with a local nematic director pointing along the wall direction is expected for finite densities. However, for active particles, we observe a novel clustering phenomenon close to the walls occurring on top of a nematization. We find an aggregation of rods at the channel walls into transiently jammed clusters which exhibit a *hedgehog-like* structure. Most of these immobile “hedgehog” clusters show up in the early stages of the aggregation process. They can efficiently block particle transport through the channel. The clusters do not only form in 2D channels but also appear in thin capillary slits in 3D. For soft particle interactions considerable homeotropic order near the walls is found which is purely generated by non-equilibrium. The aggregation near walls and the stability of hedgehog clusters is also borne out by a dynamical density functional theory which we construct from the Smoluchowski equation [15, 16, 17].

The clustering process can be detected in experiments using catalytically driven nanorods [18, 19] and colloidal particles [20] in micro-channels which exhibit the Brownian dynamics of our model [27]. A control over the hedgehog cluster formation has relevant implications for transport of active particles through confinements.

In our model, we describe a 2D system of N charged Brownian rods of length L_0 confined in a channel with a fixed width $\Delta x = 5L_0$. Rod-rod interactions are implemented via a segment model where each rod is partitioned into 13 equidistant segments [28]. Each two segments from different rods interact with each other via a

*Present address: Department of Chemical Engineering, Imperial College London, South Kensington Campus, London SW7 2AZ, United Kingdom

†Electronic address: hlowen@thphy.uni-duesseldorf.de

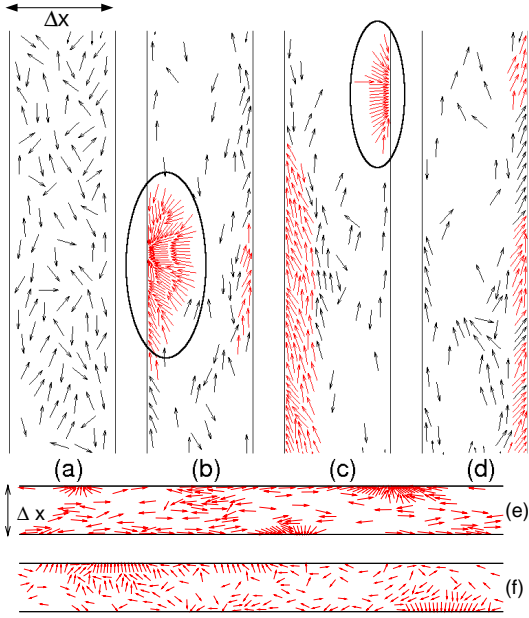


FIG. 1: (Color online) (a-d): Simulation snapshots (cutout of the full simulation box) showing the aggregation process in a 2D system of self-driven rods with $F_{\parallel} = 5k_B T/L_0$, $\kappa L_0 = 10$. (a) $t = 0$ (isotropic), (b) $t = 0.10\tau_B$ (hedgehog), (c) $t = 0.18\tau_B$ (nematized hedgehog) and (d) $t = 0.73\tau_B$ (wall aggregates). Clustered rods are shown in red, unclustered ones in black, typical hedgehog clusters are encircled. Arrows indicate the direction of F_{\parallel} . (e-f): Wall clusters appearing in a 3D slit capillary with width $\Delta x = 5L_0$ and height $\Delta z = 0.3L_0$ at the same driving force. Shown are the projections onto the xy -plane. The parameters are $\kappa L_0 = 10$, $NL_0^3/V = 5$ (with V the system volume), $t = 0.09\tau_B$ (e) and $\kappa L_0 = 5$, $NL_0^3/V = 3$, $t = 0.15\tau_B$ (f).

Yukawa potential [21]. The pair potential between two segmented rods at given center-of-mass positions $\{\mathbf{r}, \mathbf{r}'\}$ and orientational unit vectors $\{\hat{\mathbf{u}}, \hat{\mathbf{u}}'\}$ is then given by

$$U_{\text{rod}}(\mathbf{r} - \mathbf{r}'; \hat{\mathbf{u}}, \hat{\mathbf{u}}') = U_0 \sum_i \sum_j \frac{\exp[-\kappa r_{ij}]}{\kappa r_{ij}}, \quad (1)$$

with κ the Debye screening constant and $r_{ij} = |\mathbf{r} - \mathbf{r}' + (\ell_i \hat{\mathbf{u}} - \ell_j \hat{\mathbf{u}}')|$ the distance between segment i and j with $-L_0/2 < \ell_{i/j} < L_0/2$. In all cases, $U_0 = 20 k_B T$ with k_B Boltzmann's constant and T temperature. The same Yukawa segment potential is used to model the rod-wall interaction:

$$U_{\text{wall}}(x, \hat{\mathbf{u}}) = U_0 \sum_i \frac{\exp[-\kappa x_i]}{\kappa x_i}, \quad (2)$$

with $x_i = |x + \ell_i \hat{\mathbf{u}}|$ and x the rod center-of-mass distance to the channel wall. This potential prevents any particle-wall overlap and enforces the rods to orient along the channel direction.

To model an ensemble of self-propelled rods a constant force F_{\parallel} is applied along the main axis of each rod. The

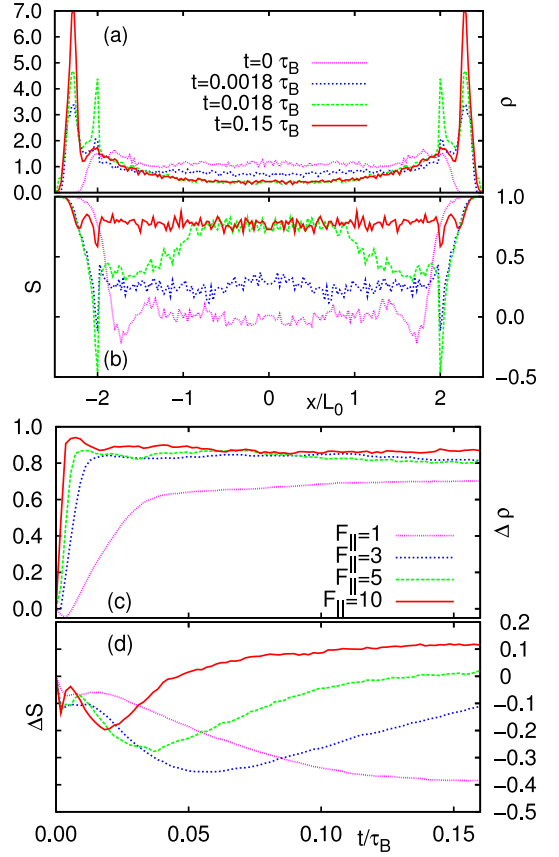


FIG. 2: (Color online) Time-dependent profiles for the number density $\rho(x)$ (a) and nematic order parameter $S(x)$ (b) for $F_{\parallel} = 10k_B T/L_0$, $\kappa L_0 = 10$ obtained from simulation. (c) Adsorption $\Delta\rho = \int_0^{L_0} [\rho(x, t) - \rho(x, 0)] dx$ and (d) excess orientation $\Delta S = \int_0^{L_0} \rho(x) [S(x, t) - S(x, 0)] dx / \int_0^{L_0} dx \rho(x)$ showing the evolution of the rod structure with respect to the equilibrium initial state near the channel walls.

system is kept at constant temperature T via the solvent and the dynamics is simulated by a finite-difference integration of the overdamped Langevin equations using the short-time translational and rotational diffusion constants of a rod taking the limit of infinite aspect ratio [21]. At any finite number density, the packing fraction of the system is then negligibly small and hydrodynamic interactions between the rods are of minor importance. The overall number density $\rho_0 = NL_0^2/A$ (with A the system area) is fixed at $\rho_0 = 1$ which corresponds to a 2D isotropic equilibrium bulk structure. Time t is measured in units of the Brownian relaxation time $\tau_B = L_0^2/D_T^{\parallel}$ of a single rod in terms of the translational diffusion coefficient parallel to the rod D_T^{\parallel} . All simulations were carried out with a time step $\delta t = 10^{-7}\tau_B$, with a periodically repeated finite system size of $125L_0$ along the channel comprising $N = 625$ rods. Rod clusters were identified using a distance criterion such that a rod pair is assigned to a cluster if their distance of closest approach is less

than κ^{-1} .

In all processes, the initial rod configuration is the isotropic equilibrium state for $F_{\parallel} = 0$. At $t = 0$, F_{\parallel} is switched to a finite value with the forces pointing randomly along the main rod axis, as depicted in Fig. 1a, and rods start accumulating at the walls forming tight clusters with a large fraction of rods pointing along the wall normal (Fig. 1b). Owing to its symmetric, semicircular shape these wall clusters will be referred to as *hedgehogs*. Since the net self-propulsion force is very small the hedgehogs are practically immobile which enables them to gather many other rods and grow rapidly. When the hedgehog has reached a certain critical size it becomes structurally unstable and slowly dissolves into a nematized cluster with nonzero cooperative motion (Fig. 1c). Simultaneously, new hedgehogs may form at a vacant part of the wall. In the steady state (Fig. 1d), the nematized hedgehogs have spread out along the walls and the rods move cooperatively in mono-layer aggregates displaying a characteristic tilt angle with respect to the wall and only few hedgehog clustering events are seen. Steady state density fluctuations are measured from $\sigma^2 = \langle M^2 \rangle - \langle M \rangle^2$ with M the number of rods in the left (L) or upper (U) half part of the simulation box. The ratios, $\sigma_L/\sigma_{L,eq} = 11$, $\sigma_T/\sigma_{U,eq} = 20$ (for $F_{\parallel} = 10k_B T/L_0$) confirm huge density fluctuations for confined driven systems.

A simulation study in a 3D slit geometry (see Fig. 1e) shows that the formation of hedgehogs is robust against the rods moving out of the 2D plane. In Fig. 1f we observe that a reduction of the effective aspect ratio κL_0 leads to a transformation of the hedgehogs into *linear homeotropic* wall clusters consisting of arrays of parallel oriented rods. These type of clusters appear to be persistent in time, also in a 3D slit-geometry. Note that the homeotropic alignment is a purely non-equilibrium effect which is not imparted by the external wall potential.

The behavior depicted in Fig. 1a-d also globally shows up in the profiles for the density $\rho(x)$ and nematic order parameter $S(x)$ across the slit, shown in Fig. 2. The latter is defined as

$$S(x) = \frac{1}{N} \sum_i \langle 1 - 2(\hat{\mathbf{u}}_i \cdot \hat{\mathbf{n}})^2 \rangle_x, \quad (3)$$

with $\langle \cdot \rangle_x$ denoting a local canonical average at position x . S is close to unity if rods are preferentially parallel to the wall, whereas a negative value indicates a favorable perpendicular alignment. The density profiles are obtained by a time-dependent canonical average of the microscopic density using about 500 independent processes. The sharp increase of the wall peak points to a strong aggregation of rods at the wall. The double peaked shape of $\rho(x)$ at intermediate times can be attributed to the presence of both hedgehogs (associated with a sharp minimum in $S(x)$) and nematized wall clusters. Details of the aggregation process are depicted in Fig. 2c-d. There, the rod structure in the direct vicinity of the walls is shown in terms of the integrated differ-

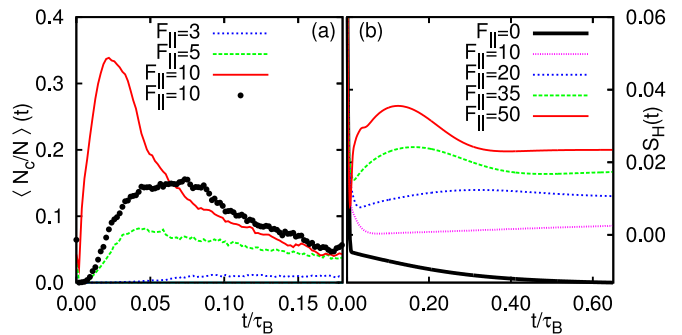


FIG. 3: (Color online) (a) Average number fraction of clustered rods (N_c/N) versus time. The solid curves correspond to an initial state of freely rotating rods, the points to an aligned state where $\hat{\mathbf{u}}_i \perp \hat{\mathbf{n}}$ for each particle i . (b) Time evolution of the hedgehog strength $\mathcal{S}_H(t)$ of a hedgehog nucleus (see Eq. (6)) from dynamical density functional theory.

ence of the profiles with respect to the equilibrium state at $t = 0$. The excess orientation (Fig. 2d) varies non-monotonically with time and the minimum can roughly be identified with the point where the transient hedgehog clusters break up and transform into nematized ones (see Fig. 1). From this we can then infer that: (1) the average lifetime of the hedgehogs becomes smaller upon increasing F_{\parallel} and (2) the ones formed at smaller driving forces have an increased propensity to be perpendicular to the wall. A similar non-monotonic behavior is encountered in the average cluster size as a function of time shown in Fig. 3. For the largest forces, the maximum appearing in the cluster fraction roughly corresponds to the ones in Fig. 2d which provides additional support for the transient clustering scenario.

We stress that at later times, say $t > 0.1\tau_B$, hedgehogs do still appear (see Fig. 1c) albeit with a smaller probability. To ensure that the qualitative features of the clustering scenario do not depend upon the initial structure, we also considered clustering starting from an equilibrated nematic system where all rods are enforced to be parallel to the wall. The result, included in Fig. 3, shows that a similar clustering process, albeit less pronounced, takes place starting from a collection of nematic swimmers.

Let us now turn to a microscopic theory for the aggregation process which is formulated in terms of the one-body density $\rho(\mathbf{r}, \hat{\mathbf{u}}, t)$ for a non-equilibrium ensemble of self-propelled rods. A general equation of motion for ρ is obtained by integrating the N -particle Smoluchowski equation which leads to [17, 22, 23]:

$$\begin{aligned} \partial_t \rho = & \nabla \cdot \mathbf{D}_T \cdot [\nabla \rho + \rho \nabla (\beta U_{\text{int}} + \beta U_{\text{wall}}) - \beta F_{\parallel} \rho \hat{\mathbf{u}}] \\ & + D_R [\partial_{\varphi}^2 \rho + \partial_{\varphi} \rho \partial_{\varphi} (\beta U_{\text{int}} + \beta U_{\text{wall}})], \end{aligned} \quad (4)$$

where $\beta = (k_B T)^{-1}$, $\nabla = \{\partial_x, \partial_y\}$ and $\hat{\mathbf{u}} = \{\sin \varphi, \cos \varphi\}$ with φ the rod-wall angle. Furthermore, \mathbf{D}_T is the diagonal translational diffusion tensor and D_R the rotational diffusion coefficient. The effective aspect ratio is fixed at

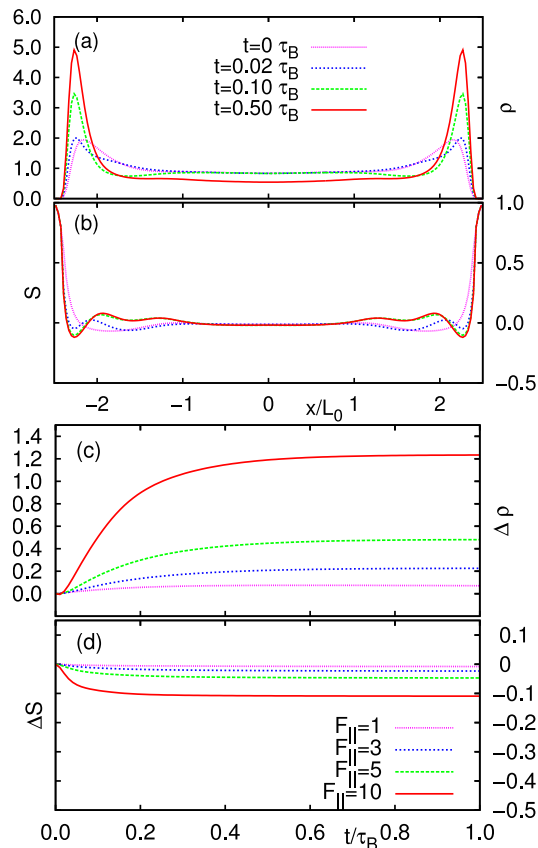


FIG. 4: (Color online) Same as Fig. 2. Results from dynamical density functional theory.

$\kappa L_0 = 10$. A connection with density functional theory is made by defining the non-equilibrium collective interaction potential $\beta U_{\text{int}} = \delta\beta F_{\text{exc}}[\rho]/\delta\rho$ in terms of the *equilibrium* excess free energy functional F_{exc} [23]. Here we use a simple Onsager functional [24, 25]

$$\beta U_{\text{int}}(\mathbf{r}, \hat{\mathbf{u}}) = - \int d\mathbf{r}' d\hat{\mathbf{u}}' (\exp[-\beta U_{\text{rod}}] - 1) \rho(\mathbf{r}', \hat{\mathbf{u}}'), \quad (5)$$

which accounts for the rod interactions on the second-virial level.

To describe the wall aggregation process we assume the density to be variable only along the wall normal $\hat{\mathbf{n}}$ and the one-body densities for $t > 0$ were numerically obtained from Eq. (4). From Fig. 4 we see that the theory captures the initial stages of the aggregation process. The growth of the wall density peak signifies a strong adsorption at the wall while the concomitant decrease of

$S(x)$ points to the rods tilting away from the wall.

To ascertain the stability of hedgehogs, we have solved Eq. (4) with full 2D spatial resolution focusing on the fate of a small semicircular hedgehog wall nucleus with radius R_c at $t = 0$ parametrized as follows:

$$\rho(\mathbf{r}, \varphi, 0) = \begin{cases} \tilde{\rho}^{eq}(x) \frac{\exp[\alpha \cos(\varphi - \gamma(\mathbf{r}))]}{2\pi I_0(\alpha)} & r < R_c \\ \rho^{eq}(x, \varphi) & r \geq R_c, \end{cases} \quad (6)$$

in terms of the local director angle $\gamma(\mathbf{r}) = \arccos(y/r) + \pi$, the equilibrium density distribution ρ^{eq} [with $\tilde{\rho}^{eq}(x) = \int d\varphi \rho^{eq}(x, \varphi)$] and local nematic order parameter $\alpha = 100$ ($I_0(\alpha)$ is a modified Bessel function). The hedgehog size can be measured in terms of the following weighted density

$$\mathcal{R}(t) = \int d\mathbf{r} d\varphi \exp[-(r/R_c)^2] \rho(\mathbf{r}, \varphi, t), \quad (7)$$

with r the distance from the center of the hedgehog nucleus at the wall. Similarly, the hedgehog *order* follows from

$$\mathcal{H}(t) = \int d\mathbf{r} d\varphi \cos(\varphi - \gamma(\mathbf{r})) \rho(\mathbf{r}, \varphi, t). \quad (8)$$

We may now define the hedgehog *strength* $\mathcal{S}_H(t) = \mathcal{R}\mathcal{H}(t)$ as a suitable parameter to assess the stability of the hedgehog nucleus over time. The result in Fig. 3b shows that a small hedgehog of size $R_c = L_0$ is indeed stabilized provided that the self-propelling force is sufficiently large. Both the transient nature of the hedgehogs and the location of the cluster maximum as a function of the force are in agreement with the simulation results in Fig. 3a.

In conclusion, we have shown that self-propelled rods confined in a channel exhibit an aggregation at the system boundaries. The aggregation process is dominated by a transient formation of virtually immobile clusters which possess a hedgehog structure. The results found in non-equilibrium Brownian dynamics computer simulations are confirmed by a microscopic dynamical density functional theory. Our predictions are in principle verifiable in experiments on colloidal suspensions [26] or catalytically driven nanorods [18, 19]. All these experimental systems are essentially realized in 2D. The aggregation phenomenon is important for blocking collective motion of active particles through narrow pores as encountered in microfluidic devices.

We thank S. Ramaswamy, S. van Teeffelen and M. Rex for helpful discussions. This work is supported by the DFG within SFB-TR6 (project D3).

- [1] T. Vicsek, A. Czirók, E. Ben-Jacob, I. Cohen, and O. Shochet, Phys. Rev. Lett. **75**, 1226 (1995).
 [2] J. Toner and Y. Tu, Phys. Rev. Lett. **75**, 4326 (1995).
 [3] H. Levine, W.-J. Rappel, and I. Cohen, Phys. Rev. E **63**,

017101 (2000).

- [4] R. A. Simha and S. Ramaswamy, Phys. Rev. Lett. **89**, 058101 (2002).
 [5] M. R. D'Orsogna, Y. L. Chuang, A. L. Bertozzi, and L. S.

- Chayes, Phys. Rev. Lett. **96**, 104302 (2006).
- [6] F. Peruani, A. Deutsch, and M. Bär, Phys. Rev. E **74**, 030904 (2006).
- [7] H. Chaté, F. Ginelli, and R. Montagne, Phys. Rev. Lett. **96**, 180602 (2006).
- [8] D. Saintillan and M. J. Shelley, Phys. Rev. Lett. **99**, 058102 (2007).
- [9] V. Narayan, S. Ramaswamy, and N. Menon, Science **317**, 105 (2007).
- [10] A. Kudrolli, G. Lumay, D. Volfson, and L. S. Tsimring, Phys. Rev. Lett. **100**, 058001 (2008).
- [11] A. Sokolov, I. S. Aranson, J. O. Kessler, and R. E. Goldstein, Phys. Rev. Lett. **98**, 158102 (2007).
- [12] D. Marenduzzo, E. Orlandini, and J. M. Yeomans, Phys. Rev. Lett. **98**, 118102 (2007).
- [13] S. Ramachandran, P. B. S. Kumar, and I. Pagonabarraga, Eur. Phys. J. E **20**, 151 (2006).
- [14] J. P. Hernandez-Ortiz, C. G. Stoltz, and M. D. Graham, Phys. Rev. Lett. **95**, 204501 (2005).
- [15] J. K. G. Dhont, *An Introduction to the Dynamics of Colloids* (Elsevier, Amsterdam, 1996).
- [16] G. Nägele, Phys. Rep. **272**, 216 (1996).
- [17] A. Baskaran and M. C. Marchetti, Phys. Rev. E **77**, 011920 (2008).
- [18] N. B. Saidulu and K. L. Sebastian, J. Chem. Phys. **128**, 074708 (2008).
- [19] P. Dhar, T. M. Fischer, Y. Wang, T. E. Mallouk, W. F. Paxton, and A. Sen, Nano Lett. **6**, 66 (2006).
- [20] M. Köppl, P. Henseler, A. Erbe, P. Nielaba, and P. Leiderer, Phys. Rev. Lett. **97**, 208302 (2006).
- [21] T. Kirchhoff, H. Löwen, and R. Klein, Phys. Rev. E **53**, 5011 (1996).
- [22] J. K. G. Dhont and W. J. Briels, J. Chem. Phys. **118**, 1466 (2003).
- [23] M. Rex, H. H. Wensink, and H. Löwen, Phys. Rev. E **76**, 021403 (2007).
- [24] L. Onsager, Ann. N.Y. Acad. Sci. **51**, 627 (1949).
- [25] A. Poniewierski and R. Holyst, Phys. Rev. Lett. **61**, 2461 (1988).
- [26] R. Dreyfus, J. Baudry, M. L. Roper, M. Fermigier, H. A. Stone, and J. Bibette, Nature **437**, 862 (2005).
- [27] Due to the solvent, the dynamics is different from granulates where inelastic collisions are important, see I. S. Aranson and L. S. Tsimring, Phys. Rev. E **71**, 050901 (2005)
- [28] Qualitatively similar results were obtained for 20 segments per rod.